

## Diffraction Behaviour of Three-Component Fibonacci Ta/Al Multilayer Films

S. S. JIANG,<sup>a</sup> R. W. PENG,<sup>a</sup> A. HU,<sup>a</sup> J. ZOU,<sup>b</sup> D. J. H. COCKAYNE<sup>b</sup> AND A. SIKORSKI<sup>b</sup>

<sup>a</sup>National Laboratory of Solid State Microstructures and Department of Physics, Nanjing University and Center for Advanced Studies in Science and Technology of Microstructures, Nanjing 210093, People's Republic of China, and

<sup>b</sup>Electron Microscope Unit, The University of Sydney, NSW 2006, Australia

(Received 5 July 1996; accepted 6 September 1996)

### Abstract

A class of quasiperiodic structure three-component Fibonacci (3CF) Ta/Al multilayer films is fabricated by dual-target magnetron sputtering. The microstructure of this film is investigated by transmission electron microscopy and electron and X-ray diffraction. Cross-section transmission electron microscopy demonstrates a well formed layer structure of 3CF Ta/Al superlattices. The electron-diffraction satellite spots, which can be indexed by three integers, correspond to the X-ray diffraction peaks in both position and intensity. The scattering vectors observed in electron and X-ray diffraction are in good agreement with the analytical treatment from the projection method.

### 1. Introduction

The quasicrystal is an intermediate state between periodic and disordered solids (Levine & Steinhardt, 1984). Since the discovery of quasicrystals by Schechtman, Blech, Gratias & Cahn (1984), considerable attention has been paid to quasiperiodic systems. In studies of quasiperiodic structures, one-dimensional (1D) quasiperiodic superlattices offer a simple example because the characteristic intervals and growth sequence can be intentionally controlled. For this reason, many experimental studies on quasiperiodic superlattices have been reported. Merlin, Bajema, Clarke, Juang & Bhattacharga (1985) were the first to produce quasiperiodic (Fibonacci) GaAs–AlAs superlattices. Since then, much progress on aperiodic superlattices has been made (Todd, Merlin & Clarke, 1986; Hu, Tien, Li, Wang & Feng, 1986). Recently, we proposed the use of quasiperiodic superlattices with high-*Z* and low-*Z* metal combinations as a reflector of soft X-rays in the case of high photon energies (Peng, Hu & Jiang 1991; Jiang *et al.*, 1992). This means that the quasiperiodic superlattices may provide optical elements for special applications and studies on quasiperiodic structures become more valuable.

While previous experiments mostly focused on the two-component quasiperiodic superlattices, we foresee a

more complicated property in reciprocal space for the three-component Fibonacci structure. The aim of this paper is to present the diffraction behaviour of three-component Fibonacci (3CF) Ta/Al superlattices by the projection method and electron and X-ray diffraction. This work is motivated by our previous studies (Peng, Hu, Jiang, Zhang & Feng 1992) of aperiodic structures with more than two components.

### 2. Theoretical model

The 3CF structure is generalized from the Fibonacci sequence with two components, *A* and *B*. This structure can be created by the substitution rule  $A \rightarrow AC$ ,  $C \rightarrow B$  and  $B \rightarrow A$ . There are several ways to describe the 3CF structure. If the limit of generation is set to be  $S_r$ , the rule  $S_r = S_{r-1} + S_{r-3}$ , with  $S_1 = \{A\}$ ,  $S_2 = \{AC\}$ ,  $S_3 = \{ACB\}$ , gives the 3CF structure. We define two ratios  $\xi$  and  $\eta$ , with  $\xi = \lim_{n \rightarrow \infty} [\text{Nr}(B)/\text{Nr}(A)]$  and  $\eta = \lim_{n \rightarrow \infty} [\text{Nr}(C)/\text{Nr}(A)]$ , where  $\text{Nr}(A)$ ,  $\text{Nr}(B)$ ,  $\text{Nr}(C)$  are the number of *A*, *B*, *C* in  $S_r$ , respectively. According to the substitution rule, these two ratios satisfy the following equations:

$$\begin{aligned} \eta^3 + \eta &= 1, \\ \eta^2 &= \xi. \end{aligned} \quad (1)$$

It follows that

$$\begin{aligned} \eta &= [1/2 + 1/2(31/27)^{1/2}]^{1/3} + [1/2 - 1/2(31/27)^{1/2}]^{1/3}, \\ \xi &= -\frac{2}{3} + [29/54 + 1/2(31/27)^{1/2}]^{1/3} \\ &\quad + [29/54 - 1/2(31/27)^{1/2}]^{1/3}. \end{aligned} \quad (2)$$

On the other hand, it is useful to recast the substitution rule in the form of a  $3 \times 3$  integer matrix *M*, *i.e.*

$$\begin{bmatrix} A \\ B \\ C \end{bmatrix} \rightarrow M \begin{bmatrix} A \\ B \\ C \end{bmatrix}, \quad (3)$$

where

$$M = \begin{pmatrix} 101 \\ 100 \\ 010 \end{pmatrix}. \quad (4)$$

Obviously, the characteristic equation of matrix  $M$  is

$$x^3 - x^2 - 1 = 0. \quad (5)$$

It is noteworthy that  $\eta$  is just reciprocal of the characteristic root  $\lambda$  of (5).

Following the Bombier–Taylor theorem, if the characteristic polynomial of the substitution rule has only one root,  $\lambda_0$ , of absolute value greater than one, *i.e.*  $\lambda_0$  is a Pisot number, the tiling will be quasiperiodic. Elser (1985) and Zia & Dallas (1985) found the projection method to generate quasiperiodic structures and dealt with the diffraction behaviour. The key of the projection method lies in the fact that a low-dimensional quasiperiodic structure may be regarded as the projection of a high-dimensional periodic structure. In the case of the 3CF structure,  $\lambda$  ( $=1/\eta$ ), as mentioned above, is a Pisot number. Therefore the 3CF structure is quasiperiodic and can be obtained by the projection method. In an orthogonal coordinate system, we project a cubic lattice along a line that satisfies

$$\cos \alpha_1 : \cos \alpha_2 : \cos \alpha_3 = 1 : \xi : \eta, \quad (6)$$

where  $\alpha_1, \alpha_2, \alpha_3$  are the angles between the projecting axis and three orthogonal coordinate axes, respectively. The set of projected points on the projected axis can construct a 3CF lattice. The three intervals  $d_A, d_B, d_C$  can be expressed as

$$d_A : d_B : d_C = \cos \alpha_1 : \cos \alpha_2 : \cos \alpha_3 = 1 : \xi : \eta. \quad (7)$$

By performance of the Fourier transformation of the real lattice, the diffraction vector  $q$  (Peng *et al.*, 1992) can be obtained:

$$q(n_1, n_2, n_3) = 2\pi D^{-1}(n_1 + n_2\xi + n_3\eta), \quad (8)$$

where  $n_1, n_2, n_3$  are integers and  $D$  is the average lattice wavelength. The diffraction peaks are located using (8). Obviously, each peak can be indexed by three indices ( $n_1, n_2, n_3$ ). The strongest peaks demonstrate the self-similarity of the reciprocal lattice, *i.e.*

$$q(a_{n+3}, a_{n+1}, a_{n+2}) = q(a_{n+2}, a_n, a_{n+1}) + q(a_n, a_{n-2}, a_{n-1}). \quad (9)$$

Here,  $a_n$  is defined as  $a_n = a_{n-1} + a_{n-3}$  with  $a_1 = a_2 = 0$  and  $a_3 = 1$ .

It should be pointed out that a cube is topologically equivalent to a cuboid. A nonstandard 3CF lattice following  $d_A : d_B : d_C \neq 1 : \xi : \eta$  can also be projected from an orthogonal lattice instead of a cubic one, and (8) and (9) still hold. This property makes it possible to realize a 3CF structure in experiments.

### 3. Experimental

The procedure to generate a 3CF structure involves two steps. First, three building blocks  $A, B, C$  are defined.

Secondly, these building blocks are ordered in the 3CF sequence. A 3CF Ta/Al multilayer film was fabricated on a glass substrate by dual-target magnetron sputtering. Fig. 1 shows the schematic layer structure of the 3CF Ta/Al film. In a typical sample, Ta slabs with the same thickness were separated by Al slabs with different thicknesses. The building blocks  $A, B$  and  $C$  consist of (11.7 Å Ta–33.64 Å Al), (11.7 Å Ta–9.13 Å Al) and (11.7 Å Ta–19.49 Å Al), respectively. The sample consists of sixteen generations of the 3CF sequence with an average lattice parameter  $D = d_A + d_B\xi + d_C\eta = 76.32$  Å, and the total thickness is  $\sim 1.44$  μm.

Cross-section specimens for transmission electron microscope (TEM) observation were prepared by ion-beam thinning. TEM observations were carried out on a Philips EM430 operating at 300 kV. The standard  $\theta$ – $2\theta$  scan of X-ray diffraction was performed using a Siemens D-2000 diffractometer with Cu  $K\alpha$  radiation and a symmetric graphite (002) monochromator.

### 4. Results and discussions

Fig. 2 shows a cross-sectional bright field image of a 3CF Ta/Al superlattice. The layer structure is well formed compared with the films prepared by the magnetron sputtering technique. The slight undulatory form

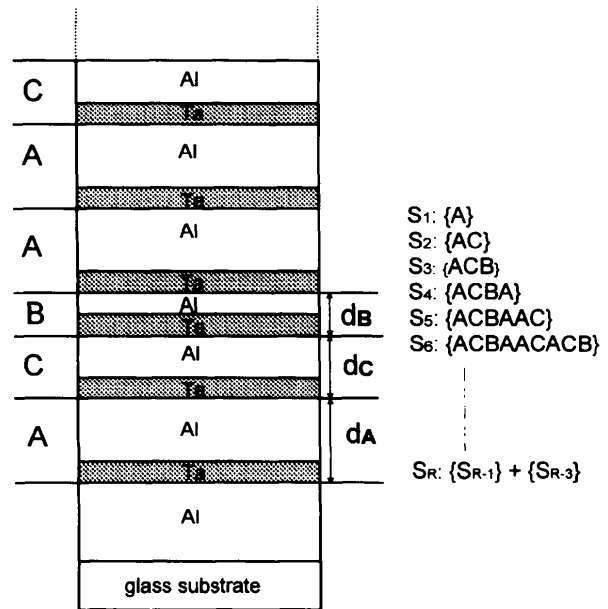


Fig. 1. Schematic ordering of three-component Fibonacci (3CF) Ta/Al multilayers. The building blocks  $A, B$  and  $C$  are (11.7 Å Ta–33.64 Å Al), (11.7 Å Ta–9.13 Å Al) and (11.7 Å Ta–19.49 Å Al), respectively. The 3CF sequence is  $ACBAACACBACBA\dots$ . The first several 3CF generations are shown. The sample consists of sixteen generations and the total thickness is  $\sim 1.44$  μm.

of the layers in the superlattice may come from the fluctuation of sputtering and the roughness of the substrate. The bright and dark layers correspond to Al and Ta slabs, respectively. The thicknesses of three building blocks are very close to the designed values, and the 3CF sequence (*ACBAACACBACBA...*) can be clearly identified.

The Fourier transform of the 3CF sequence consists of a dense set of components such that the diffraction peaks are expected at all wave vectors in the reciprocal space defined by  $q(n_1, n_2, n_3) = 2\pi D^{-1}(n_1 + n_2\xi + n_3\eta)$ . Both electron and X-ray experiments were performed on the present samples, because the microstructural information of 3CF at the local level can be obtained from electron diffraction while the information from X-ray scattering is averaged over a wide region of the 3CF sample. We can compare the experimental results from electron diffraction with those from X-ray diffraction. Fig. 3(a) shows the electron diffraction pattern of the 3CF Ta/Al superlattice (only diffraction spots on the right side of the zero beam are shown). Eight satellites are visible, and their diffraction vectors can be calculated from their spacings, and those are shown in Table 1. The corresponding X-ray diffraction spectrum of the same sample is given in Fig. 3(b). The diffraction peaks form a dense set, and their positions, intensities, diffraction vectors, as well as indexes ( $n_1, n_2, n_3$ ), are listed in Table 1. One-to-one correspondence can be found between the electron and X-ray diffraction results [shown in Fig. 3(a), (b) and Table 1] except that the first two peaks observed in the X-ray diffraction spectrum are missing in the electron diffraction pattern, probably because the zero beam of the electron diffraction pattern is too strong and swamps them. Table 1 shows that the diffraction vectors in the electron diffraction case are in good agreement with those in X-ray diffraction. The

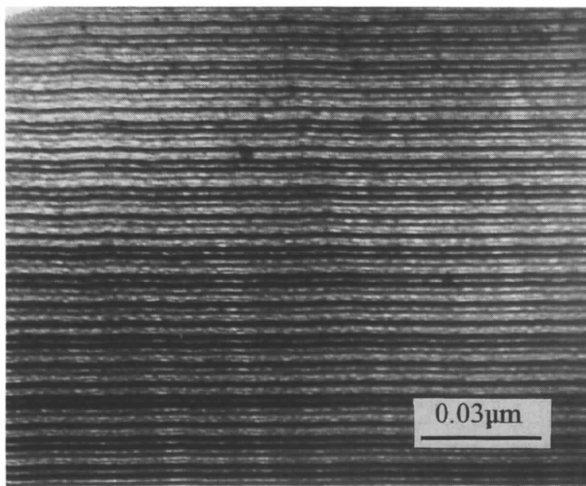
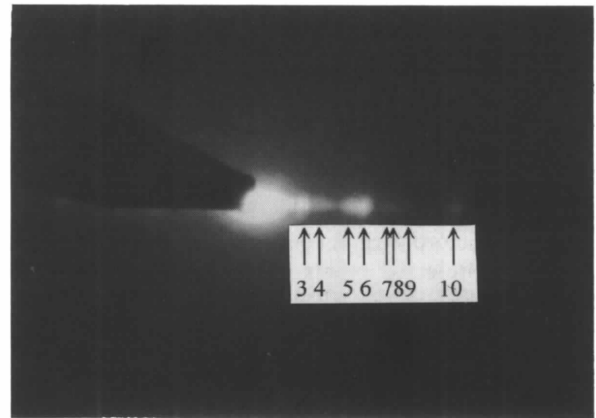


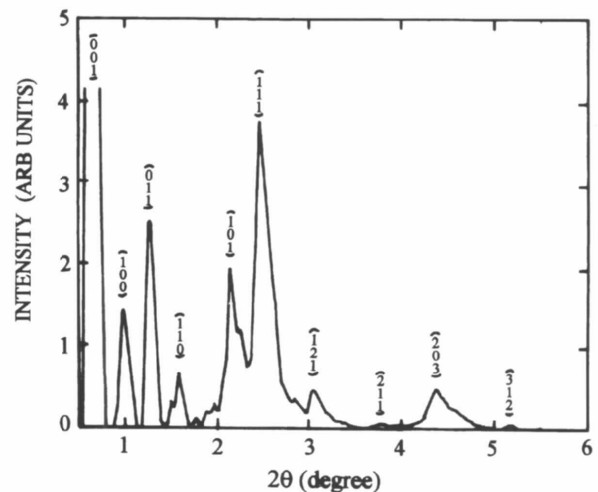
Fig. 2. The cross-sectional bright field image from 3CF Ta/Al multilayers. Ta and Al appear as dark and bright layers, respectively.

diffraction vectors in these two spectra fit the results given by equation (8). The self-similarity [shown in equation (9)] can also be found in the indices of the strong diffraction satellites. For example,  $q(3, 1, 2) = q(2, 1, 1) + q(1, 0, 1)$ .

The distribution of the spots in the electron diffraction pattern and the peaks in the X-ray diffraction spectrum from the 3CF Ta/Al superlattice are very different from the results from the periodic Ta/Al superlattice (Jiang *et al.*, 1989). In the case of the 3CF structure, the diffraction intensities do not decrease gradually when the diffraction vectors increase, as they do for the periodic Ta/Al case. The phenomenon stems from the quasi-



(a)



(b)

Fig. 3. Diffraction pattern from 3CF Ta/Al multilayers with the average lattice parameter  $D = 76.32 \text{ \AA}$ . (a) Electron diffraction pattern of cross-sectional sample near the transmitted beam. (b)  $\theta$ - $2\theta$  scan of X-ray diffraction. The strong peaks are indexed by three integers. Cu  $K\alpha$  radiation.

Table 1. *As for 3CF Ta/Al multilayer film with the average lattice parameter  $D=76.32 \text{ \AA}$ , comparison of diffraction vectors from electron and X-ray diffraction with those from the projected method*Camera length  $L\lambda=65.94 \text{ mm \AA}$  for electron diffraction. Cu  $K\alpha$  radiation for X-ray diffraction.

No.	Electron diffraction ( $q = 2\pi r/L\lambda$ )			X-ray diffraction ( $q = 4\pi \sin \theta/\lambda$ )			Indexing [ $q = 2\pi/D(n_1 + n_2\xi + n_3\eta)$ ]	
	Satellite spacing (mm)	$q$ ( $\text{\AA}^{-1}$ )	$I_{\text{obs}}$	Peak position $2\theta$ ( $^\circ$ )	$q$ ( $\text{\AA}^{-1}$ )	$I_{\text{obs}}$ (arbitrary units)	$(n_1, n_2, n_3)$	$q$ ( $\text{\AA}^{-1}$ )
1	—	—	—	0.633	$4.502 \times 10^{-2}$	32713	(0,0,1)	$5.617 \times 10^{-2}$
2	—	—	—	1.003	$7.134 \times 10^{-2}$	4206	(1,0,0)	$8.233 \times 10^{-2}$
3	0.75	0.07146	S	1.281	0.0911	7377	(0,1,1)	0.0945
4	1.20	0.1143	M	1.577	0.1121	2014	(1,1,0)	0.1207
5	1.61	0.1534	S	2.178	0.1549	5491	(1,0,1)	0.1385
6	1.90	0.1810	S	2.484	0.1767	11290	(1,1,1)	0.1768
7	2.40	0.2287	W	3.056	0.2173	1324	(1,2,1)	0.2151
8	2.80	0.2668	W	3.762	0.2675	137	(2,1,1)	0.2591
9	3.21	0.3059	W	4.376	0.3112	1383	(2,0,3)	0.3332
10	4.21	0.4011	M	5.252	0.3734	128	(3,1,2)	0.3976

periodic order. On the other hand, the locations of strong satellite spots in TEM and strong peaks in X-ray diffraction from the 3CF Ta/Al superlattice are more complicated than for Fibonacci Ta/Al multilayer films (Peng, Hu & Jiang, 1991; Jiang *et al.*, 1992), requiring labelling by three integers instead of two. As the number of components increases in 1D structures, we expect that the diffraction spectrum will become even more complicated. A transition from quasiperiodic to non-quasiperiodic diffraction behaviour may occur.

This research is supported by the National Natural Science Foundation of China. One of the authors (SSJ) wishes to thank the University of Sydney for financial support during a period of study leave spent there as a Visiting Professor.

### References

- Elser, V. (1985). *Phys. Rev. B*, **32**, 4892–4898.  
 Hu, A., Tien, C., Li, X. J., Wang, W. H. & Feng, D. (1986). *Phys. Lett. A*, **119**, 313–314.  
 Jiang, S. S., Hu, A., Chen, H., Zhang, Y. X., Qiu, Y. & Feng, D. (1989). *J. Appl. Phys.* **66**, 5258–5260.  
 Jiang, S. S., Zou, J., Cockayne, D. J. H., Sikorski, A., Hu, A. & Peng, R. W. (1992). *Philos. Mag. B*, **66**, 229–237.  
 Levine, D. & Steinhardt, P. J. (1984). *Phys. Rev. Lett.* **53**, 2477–2480.  
 Merlin, R., Bajema, K., Clarke, R., Juang, F. Y. & Bhattacharga, P. K. (1985). *Phys. Rev. Lett.* **55**, 1768–1770.  
 Peng, R. W., Hu, A. & Jiang, S. S. (1991). *Appl. Phys. Lett.* **59**, 2512–2514.  
 Peng, R. W., Hu, A., Jiang, S. S., Zhang, C. S. & Feng, D. (1992). *Phys. Rev. B*, **46**, 7816–7820.  
 Schechtman, D., Blech, I., Gratias, D. & Cahn, J. W. (1984). *Phys. Rev. Lett.* **53**, 1951–1953.  
 Todd, J., Merlin, R. & Clarke, R. (1986). *Phys. Rev. Lett.* **57**, 1157–1160.  
 Zia, R. K. P. & Dallas, W. J. (1985). *J. Phys. A*, **18**, L341–L345.